

Maderich, V., Bezhnar, R., Brovchenko, I.,
Bezhnar, A., Boeira Dias, F., & Uotila, P.
(2022). Lagrangian pathways under the
Filchner-Ronne Ice Shelf and in the Weddell Sea.
Ukrainian Antarctic Journal, 20(2), 203–211.
<https://doi.org/10.33275/1727-7485.2.2022.700>



V. Maderich^{1,*}, R. Bezhnar¹, I. Brovchenko¹,

A. Bezhnar¹, F. Boeira Dias², P. Uotila²

¹ Institute of Mathematical Machine and System Problems
of NAS of Ukraine, Kyiv, 03187, Ukraine

² Institute for Atmospheric and Earth System Research, Physics, Faculty of Science,
University of Helsinki, 00100, Finland

* Corresponding author: vladmad@gmail.com

Lagrangian pathways under the Filchner-Ronne Ice Shelf and in the Weddell Sea

Abstract. The study's objective is to construct Lagrangian pathways under the Filchner-Ronne Ice Shelf (FRIS) and in the Weddell Sea using the data of numerical simulation of currents and Lagrangian numerical methods. The results of modeling the circulation, temperature, and salinity in the Weddell Sea and the FRIS cavity from the Whole Antarctica Ocean Model were used to run the particle-tracking model (Parcels) for computing Lagrangian particle trajectories. The basic version of the Parcels model does not have an option for particle reflection from the solid boundaries, including the ice shelf. Therefore, the corresponding kernel was used in the study. To avoid errors in interpolation near the solid boundary when the model algorithm cannot find enough grid nodes around the particle, the function of particle recovery was implemented. To analyze the movement variations of the water masses under the FRIS, a set of particles was released in the Ronne Depression near the ice shelf front. Simulation continued for 20 years of particle movement. Particles were released at two depths: 350 m and 500 m, every 4 hr within the first 365 days. To characterize the redistribution of water masses, we calculated the ‘visitation frequency’, i.e., the percentage of the particles that visited each 2×2 km grid column at least once in a modeling period. The mean age of visits was also calculated to characterize the age of water masses. The results of this analysis generally agreed with schemes based on water mass analysis. The released particles first move southward along the Ronne Trough. The flow then turns to the east, reaching the passage between Berkner Island and Henry Ice Rise after three years. After ten years, the released particles reach the Filchner Trough, through which water flows out to the shelf of the southern part of the Weddell Sea. Over time, the particles penetrate all parts of the cavity. The particles also cross the Ronne Shelf front and are carried away by currents on the Weddell Sea shelf. In 20 years, almost the same number of particles left the cavity through the Ronne ice front (43%) and the Filchner ice front (37%), whereas the rest of the particles (20%) remained under FRIS.

Keywords: Filchner-Ronne Ice Shelf, High Salinity Shelf Water, Parcels model, particle trajectories, Weddell Sea, Whole Antarctica Ocean Model

1 Introduction

The Weddell Sea is an important component of the global climatic system (Vernet et al., 2019), playing an important role in forming and transporting deep waters in the Southern Ocean. A large part of the southern Weddell Sea is occupied by a huge Filchner-Ronne

Ice Shelf (FRIS). The complex circulation in the cavity under the FRIS is determined by many factors. Two main mechanisms are responsible for the formation of water masses on the Weddell Sea shelf (High Salinity Shelf Water, HSSW) and in the cavity under the FRIS (Ice Shelf Water, ISW): shelf convection and “ice pump” mechanisms (Vernet et al., 2019),

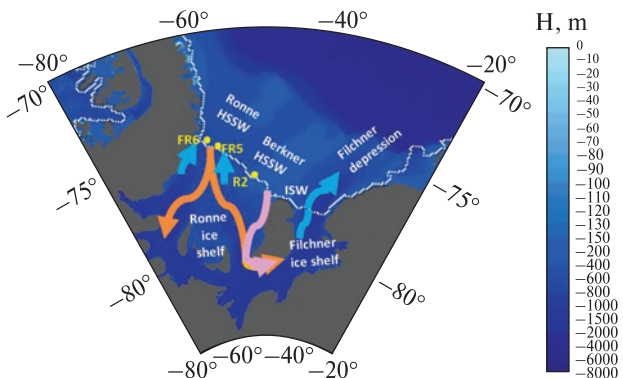


Figure 1. Map and the bathymetry of the southern Weddell Sea sector of Antarctica, showing ice shelves (white line). The sites of moorings discussed in the text (yellow labeled solid circles) and inferred from Nicholls et al. (2001; 2009), Vaňková & Nicholls (2022) water mass analysis paths of the HSSW water mass entered in Ronne Depression (orange arrow) and over Berkner Bank (light purple arrow). Blue arrows show ISW outflow

respectively. The interaction of shelf water and cavity water plays a crucial role in circulation patterns under the FRIS. However, only a few long-term measurements of currents were carried out over the last 40 years due to the difficulties of carrying out measurements under the ice shelf and its near-frontal zone. Near-ice front moorings (Foldvik et al., 2001) at two levels of the water column at site R2 on the western slope of Berkner Bank (Fig. 1) show that water can enter the cavity at a depth of about 400 m. Other moorings (FR 5 in Fig. 1) recorded currents parallel to or away from the ice front (Nicholls et al., 2003). Only mooring FR 6, on the western side of the Ronne Depression (Fig. 1), demonstrates the clear presence of the inflow of water at all depths at all times of measurements. The inflow velocity in FR 6 showed pronounced seasonal variability (Jenkins et al., 2004). The velocity into the cavity peaked in the austral summer (February), whereas in the austral winter (August), it weakened.

Two pathways for water masses entering the FRIS were identified by Nicholls et al. (2009) based on water mass analysis (Fig. 1). The inflowing HSSW through the Ronne Depression (Ronne HSSW) splits into two branches. One travels around Berkner Island, arriving as ISW at the Filchner Ice Front. The second branch

flows to the south around the Korff Ice Rise. The inflow of HSSW (Berkner HSSW) can also occur from the Berkner Bank (Foldvik et al., 2001), as suggested by the measurements in mooring R2. As seen in Figure 1, this HSSW branch flows around Berkner Island, being able to leave the Filchner Depression as ISW via the Filchner Sill (Nicholls et al., 2001). It was found (Janout et al., 2021) that the water masses in the Filchner Trough can occur in two distinct modes: Ronne HSSW-derived ISW (Ronne-mode) or more Berkner bank HSSW-derived ISW (Berkner-mode). These paths were built based on indirect data on the distribution and transformation of water masses. Therefore, it would be important to distinguish paths of the propagation of water masses using the numerical simulation data of currents and Lagrangian methods (see the review of Lagrangian ocean model analysis by van Sebille et al. (2018)). This study aims to identify the main paths using circulation model output. To perform the Lagrangian analysis, we used the simulation data on circulation in the Weddell Sea and the FRIS cavity from the Whole Antarctica Ocean Model (WAOM) described by Richter et al. (2022). The particle trajectories were computed using the modified community model Parcels (Delandmeter & van Sebille, 2019). Further analysis was carried out using the concepts of ‘visitation frequency’ (Czanady, 1983) and ‘mean age of visitation’.

2 Data and methods

2.1 Parcels model

Parcels (“Probably A Really Computationally Efficient Lagrangian Simulator”) is a framework for computing Lagrangian particle trajectories (Delandmeter & van Sebille, 2019). It is designed to process the large amount of data generated by different ocean general circulation models (OGCMs). This means that the Parcels model can work with different formats of the input fields that can be organized in large files with external data produced by OGCMs. The model includes two main components to simulate particle transport: (1) a set of interpolation schemes, and (2) special functions (kernels) to define the particle dynamics. The interpolation schemes are necessary to ob-

tain field values such as water velocities, temperature, salinity, etc., at the particle location. The movement of each particle over a certain time is calculated using 3 components of velocity at the particle location in the actual moment. External data sets from OGCM are provided to Parcels as a set of fields. Each field is discretized on a structured grid that provides the node locations and times of the recordings. A detailed description of interpolation schemes for different types of OGCM model grids is given by Delandmeter and van Sebille (2019).

In the Parcels model, some basic kernels are available, and others could be developed by the user. For example, three options are available for the simulation of the advection. They are the fourth-order Runge–Kutta, Runge–Kutta–Fehlberg, and explicit Euler integration schemes. Kernels for constant and spatially varying horizontal diffusion are also available. In addition, particle data can save values of different fields (e.g., traveled distance, temperature, salinity) along the particle trajectory. The model's source code is licensed under an open-source MIT license and can be downloaded from github.com/OceanParcels/parcels to be installed via anaconda.org/conda-forge/parcels. The detailed instruction for the installation is on the website: <http://www.oceanparcels.org>.

The basic version of the Parcels model does not have an option for particle reflection from the solid boundaries, including the ice shelf. The corresponding kernel was implemented in the study to reflect the particle from the solid boundary. However, such reflections near boundaries of a complicated form can lead to a situation when the particle becomes “out of boundary”. Usually, it can happen on the ice shelf boundary where the vertical position of neighboring grid nodes may differ by tens of meters due to the sigma system of coordinates used in the circulation model. This causes the particle to disappear as a result of the interpolation error when the model algorithm cannot find enough grid nodes around the particle.

Particle loss is a known problem of Lagrangian models: e.g., about 30% of released particles were lost to advection into topography (Tamsitt et al., 2017). Therefore, a kernel preventing the loss of particles was developed and applied. This kernel recovers the particle

in the location of its last valid coordinate before it disappears with a small random variation in three dimensions: $d\lambda$ (longitude), $d\phi$ (latitude), and dz (depth). If the particle disappeared again, the kernel was also applied again until the particle continued its movement in the field of currents. Such an algorithm slightly slows down the calculations but it provides conservation of the number of particles.

Small random deviations of particle location allowed the particle to find a position where the vector of currents was slightly different to go around the curved boundary. The amplitudes of random deviations were chosen as 1/2 of the grid size in the horizontal direction and 1 m in the vertical direction. Deviations in three dimensions were used because the geometry of the ice shelf boundary changes in three dimensions: the ice boundary can propagate from the surface to some depth, whereas the water column is placed between the ice shelf and the bottom. The applied algorithm was tested to check how much the trajectory can change due to random deviations. For this aim, a number of particles were released from the same point simultaneously, and their trajectories were analyzed. The developed algorithm could change the trajectory of the individual particle but not impact the statistical characteristics such as visitation frequency when a large number of particles are released. Standard Parcels functions for calculating particle distance traveled and field sampling along the particle trajectories (Delandmeter & van Sebille, 2019) were also applied in the study.

2.2 Model setup

Output from the WAOM simulation includes three components of velocity (U , V , W), potential temperature (T), water salinity (S), bathymetry (H), sea elevation (η), ice shelf draft (z_{ice}), horizontal coordinates for nodes of computation grid (λ , ϕ), and vertical sigma-coordinates at computation levels (σ). The spatial resolution of provided data is in the range of 2 to 10 km. The model domain covers the circum-Antarctica region. The temporal resolution of fields of U , V , W , η , T , and S is five days. We used one year (365 days) of output. The Parcels model requires z coordinates in

the vertical direction. Therefore sigma-coordinates were converted to z -coordinates using data of H , η , and z_{ice} . All data sets from the WAOM model were cycled (i.e., the yearly data were repeated).

To analyze the variations of movement of the water masses under the FRIS, a set of particles was released in the Ronne Depression near the ice shelf front. The geographical coordinates of the release point were 75.15°S and 61.4°W. This release location (inverted white triangle in Fig. 2a) was chosen because only in the region of the Ronne Depression is a clear observed flux of water directed further under the ice shelf (Jenkins et al., 2004). Particles were released at 350 m and 500 m under the sea surface. Both release depths were placed under the ice shelf front. Particles were released each 4 hr within 365 days. In total, 2190 particles were released at each depth. Below we present only simulation results for a release depth of 350 m because using a release depth of 500 m results in a similar distribution of particles. Simulation continued for 20 years of particle movement. The Runge-Kutta fourth-order method was used. The time step of the simulation was 3 min. Such a small step was chosen to take into account the relatively high resolution of the WAOM grid under the ice shelf and to reduce the number of cases where particles can escape from the computational domain solid boundary.

3 Results

The individual particle trajectories are complicated and provide only an illustration of the pattern of transport processes. To characterize the redistribution of Lagrangian particles by currents in the simulation domain, we calculated ‘visitation frequency’ (Csanady, 1983) which is the percentage of the particles P that visit each 2×2 km grid column at least once in a period of modeling (20 y). If all particles visited the given area bin then $P = 1$ whereas in case there are no visits, $P = 0$. To quantitatively describe the transport by particles, it is necessary to apply a different approach (e.g., Drake et al., 2018; van Sebille et al., 2018) which is beyond the scope of this article. The results of the calculation of P are given in Figure 2a. As seen in Figure 2a, the released particles first move southward along the Ronne Trough. The flow then turns to the northeast and east reaching the passage between Berkner Island and Henry Ice Rise. Then the flow reaches the Filchner Trough through which water flows out to the shelf of the southern part of the Weddell Sea. Besides, particles penetrate all parts of the cavity (Fig. 2a). Unexpectedly, a strong flow across the Ronne Shelf front and further across the Weddell Sea shelf was visible in the visitation frequency map. Its presence, however, is consistent with

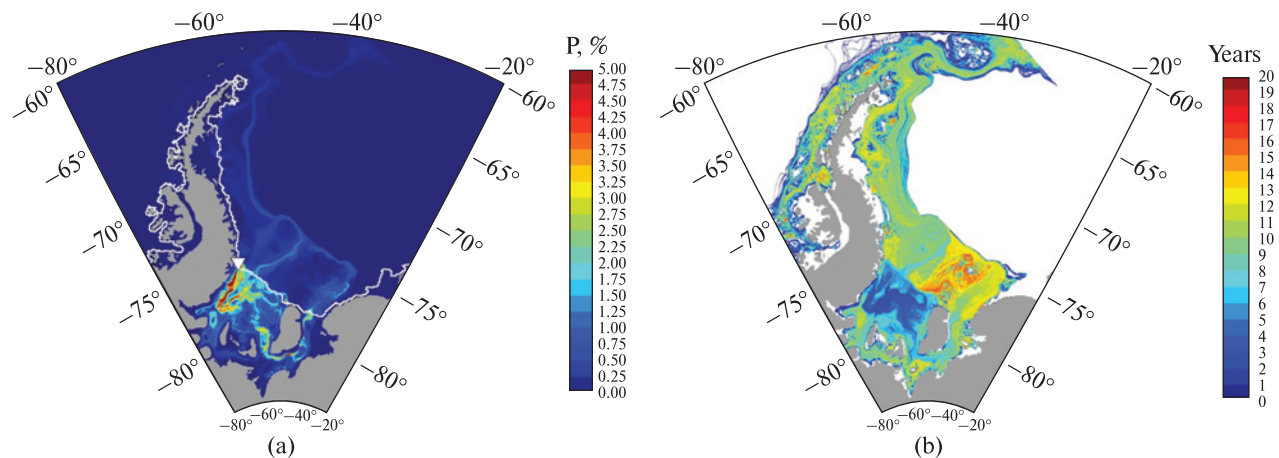


Figure 2. Visitation frequency defined as the percentage of the particles P visited each 2×2 km grid column at least once (a). The release point in Figure 2a is indicated by an inverted white triangle. The mean age of particles that visited each 2×2 km grid column at least once (b). The ice shelf fronts are shown by the white line

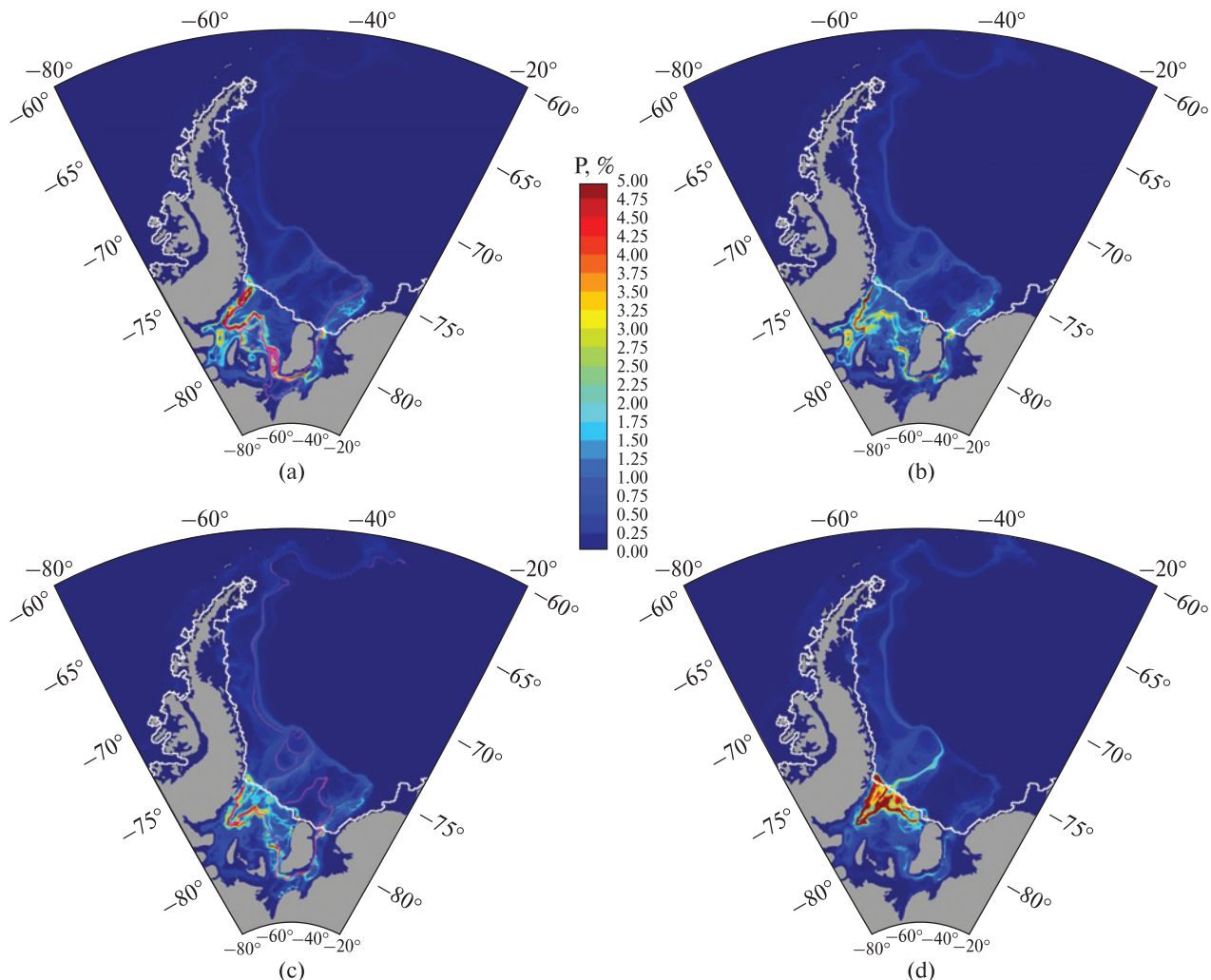


Figure 3. Visitation frequency for particles released in December–February (a), March–May (b), June–August (c), and September–November (d). Examples of individual trajectories for winter (a) and summer (c) are shown in purple lines

the measurements at st. FR5 (Nicholls et al., 2003) and scheme of water mass transport (Vaňková & Nicholls, 2022). Then particles are carried away by currents on the Weddell Sea shelf. Further particle flow splits into two at the tip of the Antarctic Peninsula. In one case, particles move eastward into the Scotia Sea, and the second much weaker flow ($P < 0.5\%$) turns westward into the Bellingshausen Sea moving along the coast of the Western Antarctic Peninsula.

In 20 years, almost the same number of particles left the cavity through the Ronne ice front (43%) and the Filchner ice front (37%), whereas the rest of the particles

(20%) remained under the FRIS. Changes in particle distribution with time resulting in visitation frequency in Figure 2a generally correspond to the scheme of water mass movement under the FRIS in Figure 1. The HSSW water mass moves to the southeast and leaves the FRIS through the Filchner Trough as ISW. The difference from the scheme in Figure 1 is that there is no source of lighter HSSW water on the Berkner Rise. The simulation results correspond to the Ronne HSSW-derived ISW (Ronne-mode, according to Janout et al. (2021)).

Another useful statistical information is the mean age of particles that visited each 2×2 km grid column

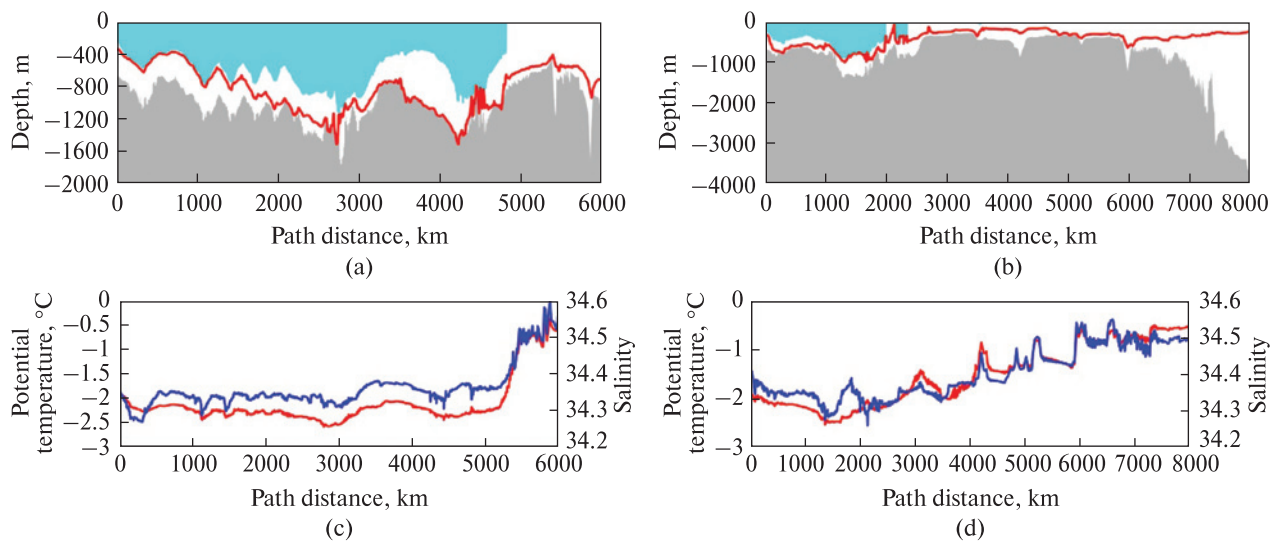


Figure 4. (a) Vertical section of the water column between the ice shelf (cyan) and the bottom (grey) along the trajectory (red line) of a particle released in February at a depth of 350 m; (b) vertical section of the water column between the ice shelf and the bottom along the trajectory (red line) of a particle released in August at a depth of 350 m; (c) variations of potential temperature (red line) and salinity (blue line) along the path of particle released in February at a depth of 350 m; (d) variations of potential temperature (red line) and salinity (blue line) along the path of particle released in August at a depth of 350 m

at least once. As seen in Figure 2b, in the northern part of the Ronne Ice Shelf, the average age of the waters is relatively small (less than 6–7 years). Note the presence of a stagnant deep-water pool of older water (age about 11–12 years) between the Korff Ice Rise and the mainland in the west (about 12 years old). It is also observed as a local maximum visitation frequency in Figure 2a. The mean age of visitation frequency increases in the Filchner Depression to 7–10 years. On the shelf opposite Berkner Island, a large pool of waters aged from several years to 15–16 years is formed due to a complex pattern of currents in this area. It is necessary to note the inflow of relatively young waters to the shelf from under the Ronne Ice Shelf, which is visible in Figure 2a.

Figure 3 shows visitation frequency maps built for particles released in the same location (see Fig. 2a) in austral summer (December, January, February), autumn (March, April, May), winter (June, July, August), and spring (September, October, November) at a depth of 350 m. In general, these maps are similar to Figure 2a. However, some important differences between Figure 2a and Figure 3 demonstrate season-

al effects. In January-August, water outflows occurred through both the Ronne and Filchner ice fronts, as suggested by visitation frequency maps. In October-December, water outflow through the Ronne ice front essentially exceeded the water flow through the Filchner Depression.

Vertical sections of the water column between the ice shelf base and the bottom along the trajectory of a particle released in austral summer (15 February 12.00 a.m.) and winter (15 August 12.00 a.m.) at a depth of 350 m are shown in Figures 4a and 4b. These trajectories are shown in Figure 3a and 3c by pink lines. The corresponding variations of potential temperature and salinity along the path of the particle are given in Figures 4c and 4d. The particle paths follow the topography of the bottom and lower surface of the ice shelf. As seen in Figures 4c and 4d, variations of the potential temperature in particles moving under the ice shelf were essentially compensated by variations of salinity. At the same time, as seen in Figure 4, outside the FRIS cavity, temperature and salinity can vary significantly due to interaction with the atmosphere on the shelf of the Weddell Sea.

4 Conclusions

The Lagrangian pathways under the FRIS and in the Weddell Sea were studied using the data of numerical simulation of currents from the Whole Antarctica Ocean Model (WAOM) model and the particle-tracking Parcels model. The new kernels were added to the Parcels to improve the numerical realization of the boundary conditions on solid boundaries of the computational domain, including the ice shelf. A set of particles was released in the Ronne Depression near the ice front to track water mass movement over 20 years. This location was chosen because a clear flux of HSSW directed to the Ronne Ice Shelf was observed only here. The corresponding flux of Berkner HSSW was not identified in the simulations. The visitation frequency, defined as the percentage of particles that visited each 2×2 km grid column at least once in a period of modeling, was calculated for the first time to characterize the redistribution of water masses under the FRIS and in the Weddell Sea. The results of this analysis generally agreed with schemes based on water mass analysis (Nicholls et al., 2009; Vaňková & Nicholls, 2022). The results of simulations show that the particles released in the Ronne Depression near the ice shelf front first move southward along the Ronne Trough.

The flow then turns to the east, reaching the passage between Berkner Island and Henry Ice Rise after three years. After ten years, the water reaches the Filchner Trough and flows out to the shelf of the southern part of the Weddell Sea. Over time, the particles penetrate all parts of the cavity. The strong flow across the Ronne Shelf front and further across the Weddell Sea shelf was visible in the visitation frequency map. This is consistent with measurements at st. FR5 and scheme of water mass transport under the Ronne Ice Shelf (Vaňková & Nicholls, 2022). The difference from the scheme in Figure 1 is that there is no source of lighter HSSW water on the Ice Rise on Berkner Island that corresponds to Ronne-mode circulation (Janout et al., 2021). In 20 years, almost the same number of particles left the cavity through the Ronne ice front (43%) and the Filchner ice front (37%), whereas the rest of the particles (20%) remained under FRIS.

Passing through the Weddell Sea shelf, particle flow splits in two at the end of the Antarctic Peninsula. In one case, particles move eastward into the Scotia Sea. The second, much weaker flow ($P < 0.5\%$) turns westward into the Bellingshausen Sea, moving along the coast of the Western Antarctic Peninsula. The mean age of particles that visited each 2×2 km grid column was calculated at least once. The visitation age increased for values less than 6–7 to 15–16 years on the shelf opposite Berkner Island. The seasonal effects were also found. They are visible in visitation frequency maps in Figure 3, drawn for particles released in the same location at four seasons. In January-August, outflows took place through both the Ronne and Filchner ice fronts, as suggested by visitation frequency maps. In October-December, outflow through the Ronne ice front exceeded the flow through the Filchner Depression.

Author contribution. V. M., P. U.: conceptualization. R. B., I. B.: numerical modeling. R. B., A. B., F. B. D.: data processing. V. M., I. B., A. B.: data analysis. V. M., R. B.: writing – original draft. I. B., F. B. D., P. U.: writing – review, and editing.

Acknowledgments. This work was supported by the European Union's Horizon 2020 research and innovation framework program (Polar RES, Grant Agreement 101003590).

Conflict of Interest. The authors declare that they have no conflict of interest.

References

- Csanady, G. T. (1983). Dispersal by randomly varying currents. *Journal of Fluid Mechanics*, 132, 375–394. <https://doi.org/10.1017/S0022112083001664>
- Delandmeter, P., & van Sebille, E. (2019). The Parcels v2.0 Lagrangian framework: new field interpolation schemes. *Geoscientific Model Development*, 12(8), 3571–3584. <https://doi.org/10.5194/gmd-12-3571-2019>
- Drake, H. F., Morrison, A. K., Griffies, S. M., Sarmiento, J. L., Weijer, W., & Gray, A. R. (2018). Lagrangian timescales of Southern Ocean upwelling in a hierarchy of model resolutions. *Geophysical Research Letters*, 45(2), 891–898. <https://doi.org/10.1002/2017gl076045>
- Foldvik, A., Gammelsrød, T., Nygaard, E., & Østerhus, V. (2001). Current measurements near Ronne Ice Shelf: Impli-

- cations for circulation and melting. *Journal of Geophysical Research: Oceans*, 106(C3), 4463–4477. <https://doi.org/10.1029/2000JC000217>
- Janout, M. A., Hellmer, H. H., Hattermann, T., Huhn, O., Sütlenfuss, J., Østerhus, S., Stulic, L., Ryan, S., Schröder, M., & Kanzow, T. (2021). FRIS revisited in 2018: On the circulation and water masses at the Filchner and Ronne ice shelves in the southern Weddell Sea. *Journal of Geophysical Research: Oceans*, 126(6), e2021JC017269. <https://doi.org/10.1029/2021JC017269>
- Jenkins, A., Holland, D. M., Nicholls, K. W., Schröder, M., & Østerhus, S. (2004). Seasonal ventilation of the cavity beneath Filchner-Ronne Ice Shelf simulated with an isopycnic coordinate ocean model. *Journal of Geophysical Research: Oceans*, 109(C1), C01024. <https://doi.org/10.1029/2001JC001086>
- Nicholls, K. W., Østerhus, S., Makinson, K., & Johnson, M. R. (2001). Oceanographic conditions south of Berkner Island, beneath Filchner-Ronne Ice Shelf, Antarctica. *Journal of Geophysical Research: Oceans*, 106(C6), 11,481–11,492. <https://doi.org/10.1029/2000JC000350>
- Nicholls, K. W., Padman, L., Schröder, M., Woodgate, R. A., Jenkins, A., & Østerhus, S. (2003). Water mass modification over the continental shelf north of Ronne Ice Shelf, Antarctica. *Journal of Geophysical Research: Oceans*, 108(C8), 3260. <https://doi.org/10.1029/2002JC001713>
- Nicholls, K. W., Østerhus, S., Makinson, K., Gammelsrød, T., & Fahrbach, E. (2009). Ice-ocean processes over the continental shelf of the southern Weddell Sea, Antarctica: A review. *Reviews of Geophysics*, 47(3), RG3003. <https://doi.org/10.1029/2007RG000250>
- Richter, O., Gwyther, D. E., Galton-Fenzi, B. K., & Naughten, K. A. (2022). The Whole Antarctic Ocean Model (WAOM v1.0): development and evaluation. *Geoscientific Model Development*, 15(2), 617–647. <https://doi.org/10.5194/gmd-15-617-2022>
- Tamsitt, V., Drake, H. F., Morrison, A. K., Talley, L. D., DuFour, C. O., Gray, A. R., Griffies, S. M., Mazloff, M. R., Sarmiento, J. L., Wang, J., & Weijer, W. (2017). Spiraling pathways of global deep waters to the surface of the Southern Ocean. *Nature Communications*, 8, 172. <https://doi.org/10.1038/s41467-017-00197-0>
- van Sebille, E., Griffies, S. M., Abernathey, R., Adams, T. P., Berloff, P., Biastoch, A., Blanke, B., Chassignet, E. P., Cheng, Y., Cotter, C. J., Deleersnijder, E., Döös, K., Drake, H. F., Drijfhout, S., Gary, S. F., Heemink, A. W., Kjellsson, J., Koszalka, I. M., Lange, M., ... & Zika, J. D. (2018). Lagrangian ocean analysis: fundamentals and practices. *Ocean Modelling*, 121, 49–75. <https://doi.org/10.1016/j.ocemod.2017.11.008>
- Váňková, I., & Nicholls, K. W. (2022). Ocean variability beneath the Filchner-Ronne Ice Shelf inferred from basal melt rate time series. *Journal of Geophysical Research: Oceans*, 127(10), e2022JC018879. <https://doi.org/10.1029/2022JC018879>
- Vernet, M., Geibert, W., Hoppema, M., Brown, P. J., Haas, C., Hellmer, H. H., Jokat, W., Jullion, L., Mazloff, M., Bakker, D. C. E., Brearley, J. A., Croot, P., Hattermann, T., Hauck, J., Hillenbrand, C.-D., Hoppe, C. J. M., Huhn, O., Koch, B. P., Lechtenfeld, O. J., ... & Verdy, A. (2019). The Weddell Gyre, Southern Ocean: Present knowledge and future challenges. *Reviews of Geophysics*, 57(3), 623–708. <https://doi.org/10.1029/2018RG000604>

Received: 13 October 2022

Accepted: 2 February 2023

**В. Мадерич^{1,*}, Р. Беженар¹, І. Бровченко¹,
А. Беженар¹, Ф. Боєйра Діас², П. Уотіла²**

¹ Інститут проблем математичних машин і систем НАН України,
м. Київ, 03187, Україна

² Інститут досліджень атмосферних і земних систем,
університет Хельсінкі, м. Хельсінкі, 00100, Фінляндія

* Автор для кореспонденції: vladmad@gmail.com

**Лагранжеві шляхи під шельфовим льодовиком Фільхнера-Ронне
та в морі Ведделла**

Реферат. Метою дослідження є побудова лагранжевих шляхів руху водних мас під шельфовим льодовиком Фільхнера-Ронне (FRIS) і в морі Ведделла з використанням даних чисельного моделювання течій і чисельних лагранжевих методів. Результати моделювання циркуляції, температури та солоності в морі Ведделла та під льодовиком FRIS, отримані за допомогою моделі Whole Antarctica Ocean Model (WAOM), були використані для запуску моделі відстеження траекторій частинок Parcels. Оригінальна версія моделі Parcels не має опції відбиття частинок від твердих меж, включаючи шельфовий льодовик. Тому в даному дослідженні було розроблено відповідну функцію. Модель Parcels дає помилку в інтерполяції, коли не може знайти достатньо вузлів сітки навколо частинки. Щоб уникнути цієї помилки, було розроблено функцію відновлення частинок в місці зникнення з невеликою випадковою варіацією в трьох вимірах. Щоб проаналізувати варіації руху водних мас під FRIS, набір частинок був випущений у западині Ронне по-

блізу фронту шельфового льодовика. Випуск частинок відбувався на двох глибинах: 350 м і 500 м. Частинки з'являлися в одній точці кожні 4 години протягом 365 днів. Моделювання тривало протягом 20 років руху частинок. Результати лагранжевого аналізу загалом узгоджувалися зі схемами, заснованими на аналізі водних мас. Випущені частинки спочатку рухаються на південь уздовж жолоба Ронне. Потім потік повертає на схід, досягаючи проходу між островом Беркнера і підняттям Генрі через 3 роки. Через 10 років потік трансформованої води досягає жолоба Фільхнера, через який вода витікає на шельф південної частини моря Ведделла. З часом частинки проникають у всі частини порожнин під льодовиком. Частина частинок перетинає фронт шельфу Ронне, а потім виноситься течіями на шельф моря Ведделла. За 20 років майже однакова кількість частинок залишила порожнину через льдовий фронт Ронне (43%) і льдовий фронт Фільхнера (37%), тоді як решта (20%) залишилися під FRIS.

Ключові слова: Whole Antarctica Ocean Model, льодовик Фільхнера-Ронне, модель Parcels, море Ведделла, траєкторія частинок, шельфова вода високої солоності